Surface & Coatings Technology 231 (2013) 399–402

Contents lists available at ScienceDirect

Surface & Coatings Technology

journal homepage: www.elsevier.com/locate/surfcoat

Resistive switching behavior of sol–gel deposited TiO_2 thin films under different heating ambience

Chun-Hung Lai [a,*], Chia-Hung Chen [b], Tseung-Yuen Tseng [b]

[a] Department of Electronic Engineering, National United University, Miaoli 360, Taiwan
[b] Department of Electronics Engineering and Institute of Electronics, National Chiao Tung University, Hsinchu 300, Taiwan

ARTICLE INFO

Available online 26 May 2012

Keywords:
Anatase
Sol–gel
Resistive switching
XPS

ABSTRACT

We prepared anatase TiO_2 films by sol–gel method under three thermal firing conditions to investigate the bipolar resistive switching (BRS) and unipolar resistive switching (URS) in Ag/TiO_2/Pt structure. The devices are URS in an air atmosphere at 760 Torr, while those in an oxygen ambience at 1 Torr show BRS accompanying with forming-free and self-compliance. By examining the X-ray photoelectron spectroscopy (XPS) spectrum, different non-lattice oxygen content is observed. High concentration of oxygen vacancy is expected under oxygen-deficient treatment, and that would determine the electrode/oxide interface property and induce switching mode of polarity dependent or not. An improved performance of operation voltage dispersion down to 0.5 V and endurance up to 3000 cycles is obtained for those in reducing Ar.

1. Introduction

Transition metal oxide (TMO)-based resistive random-access memories (RRAMs) have been studied as next-generation nonvolatile memory due to their simple cell structure, fast switching speed, low power consumption, long retention, and high endurance [1–3]. Scientists often explain the resistive switching behavior between the two level resistance states in TMO-based RRAMs by the formation and rupture of conduction filament [4–6], in which the transition from high resistance state (off-state) to low resistance state (on-state) is called the set process, and the opposite operation is called the reset process. Most RRAM devices require a forming process before showing the resistive switching (RS) behavior. Depending on whether set and reset processes are of the same voltage polarity, the RS mode could be classified as unipolar (URS) or bipolar (BRS). Schroeder et al. discovered that Pt/TiO_2/Pt shows URS and BRS by setting forming process of different compliance current (I_{cc}) [7]. Choi et al. found a consequence of URS and BRS for TiO_2 with Pt or Ti top electrode [2]. Zhang demonstrated the reversible and controllable conversion between URS and BRS in Pt/TiO_2/Pt by changing the operation method [8]. Yu et al. proposed a switching model by simulating the existence of an interfacial barrier in oxidizable electrode materials, which is absent in noble electrode materials [9]. In all the binary or ternary metal oxides with RS property, oxygen vacancy is widely accepted by the filamentary model to explain the ret/reset transition [8,9]. This study examines the effect of three oxygen-containing atmosphere treatments on electrical properties, and elucidates the resultant URS and BRS switching modes accordingly. Endurance comparison between them is also made and discussed.

2. Experiment

The 0.4 M precursor solution of TiO_2 was prepared by dissolving the titanium isopropoxide (TTIP) in an ethanol solvent. The reaction rate of the hydrolysis and polycondensation was adjusted by using the hydrochloric acid and deionized water as activators. The mixture mole ratio of TTIP, hydrochloric acid, and deionized water was 1:0.82:0.13 [10]. The as-grown TiO_2 thin films were then deposited on the Pt/Ti/SiO_2/Si substrate by repeating spin-coating and preheating twice. The two-step spin-coating procedure was adopted to enhance the uniformity, the first being 1000 rpm for 10 s and the second being 2000 rpm for 30 s. By a rising rate of 10 °C/min to 110 °C, the pre-treatment was performed for 60 min to remove the solvent and activators. The TiO_2 thin films were formed at 350 °C in a furnace under three different conditions: an air atmosphere at 760 Torr (air_760Torr), an oxygen atmosphere at 1 Torr (O_2_1Torr), and an argon atmosphere of 1 Torr (Ar_1Torr). The 350 °C was the lowest temperature in series of tests for samples with resistance switching property. Finally, the 250 nm-thick silver was evaporated as the top electrode, and the electrode of 100 μm diameter was patterned with a shadow mask. The Ag top electrode could also serve as an aid to filament formation via interstitial ionic diffusion in the TiO_2 matrix. The cross-sectional morphology of the Ag/TiO_2/Pt sandwiched structure was obtained using a scanning electron microscope (SEM, Jeol 5600). All the electrical characteristics were measured using a

* Corresponding author.
E-mail address: brandon@nuu.edu.tw (C.-H. Lai).

0257-8972/$ – see front matter © 2012 Elsevier B.V. All rights reserved.
doi:10.1016/j.surfcoat.2012.05.045

semiconductor parameter analyzer (SPA, Agilent 4155A) in voltage sweep mode. The crystalline structure and composition of the TiO_2 thin films were investigated by X-ray diffraction (XRD, Rigaku RUH3R) and X-ray photoelectron spectroscopy (XPS, Jeol JAMP9500F).

3. Results and discussion

Fig. 1(a) shows the XRD patterns for three sets of samples. All the TiO_2 films show the strongest anatase (101) peaks, and the peaks for Pt bottom electrode and Ti adhesion layer are also observed [11,12]. Non-stoichiometric TiO_x with intrinsic oxygen vacancy was commonly reported in the literature. It is speculated that the anatase structure does not have sufficient oxygen ions to bond with Ti, and therefore generating the non-lattice oxygen generally found in the XPS analysis. Fig. 1(b) shows the uniform and smooth quality of 200 nm-thick TiO_2 thin films prepared by sol–gel method. Under the same firing temperature but different oxygen availability, a decreasing grain size around 15/7/5 nm, based on the SEM images, is found for air, O_2 and Ar samples respectively. Due to high current leakage (>100 mA), the resistive switching characteristic was not found for films of thickness lower than 200 nm.

Fig. 2(a) shows the air_760Torr URS and its subsequent 10th and 100th curves. The initial un-formed device is in insulating state. Typically for URS, an electrical-forming process is required to activate the devices into the on-state by generating conducting filaments through the TiO_2 films. The inset shows that the forming voltage $V_{forming}$ is approximately −3.5 V. The set process is conducted by negative sweeping. The current increases smoothly at lower bias, and a sudden jump in current occurs at the threshold (V_{set}, I_{set}). V_{set} is in the range of −1.2 V to −2.4 V by successive I–V measurements. Current compliance I_{cc} of 10 mA is set to avoid hard breakdown in forming and set processes.

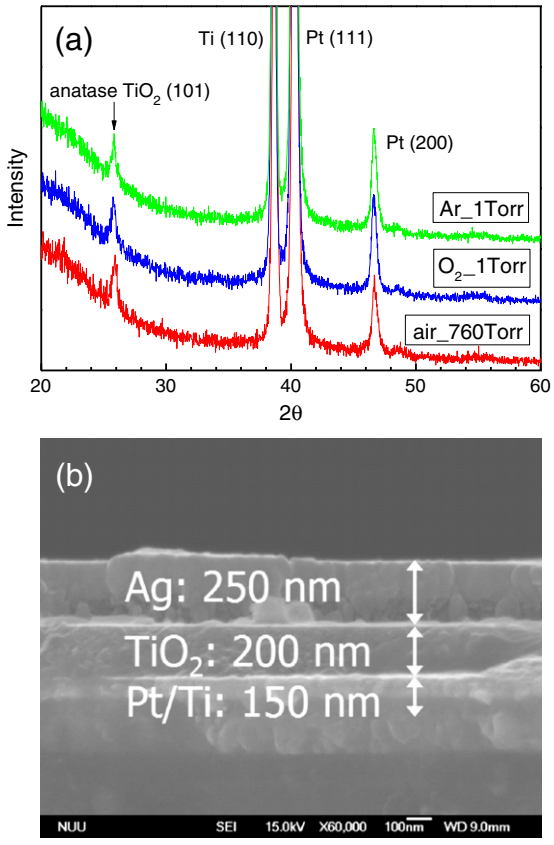

Fig. 1. (a) XRD patterns for three sets: air_760Torr, O2_1Torr and Ar_1Torr, (b) the typical cross-section SEM image for air_760Torr.

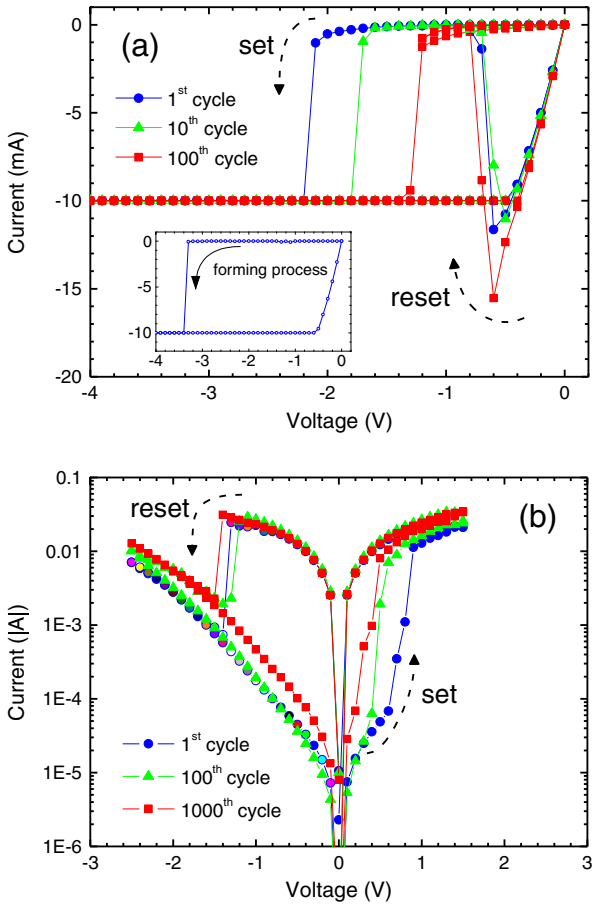

Fig. 2. I–V characteristics (a) for air_760Torr URS in a continuous switch of 100 times. The inset is the forming process, (b) for O2_1Torr BRS in a continuous switch of 1000 times.

For O_2_1Torr in Fig. 2(b), by contrast, the device displays BRS with forming-free and self-compliance features. The as-deposited film in most cases is in its off state, and forming-free indicates the presence of pre-existing, but not active, conduction path. Or one can say $V_{forming}$ is close to V_{set} when turning on the initial state. It is found that forming-free devices show more stable RS characteristics than the forming-necessary ones [10], and usually those BRS devices with abundant oxygen vacancies possess this feature [13]. An improved uniformity of device parameters and better endurance is obtained in those with self-compliance, which could be attributed to the uniform on-state resistance [14]. V_{set} is only 0.1 V–0.8 V. The apparent asymmetric branches are observed in positive and negative bias. Since RRAM devices store 1/0 by distinct resistance in high and low conduction states, it won't make operation errors in present case.

The dependence of reset currents I_{reset} on the compliance setting I_{cc} could be interpreted based on filament model [11,15]. Fig. 3 shows a larger I_{reset} by increasing I_{cc} for both URS and BRS. A higher I_{cc} implies the possibility of increasing number, size, or density of conductive filaments generated in the turn-on process. This would reasonably require larger current to rupture them. By adjusting I_{cc}, one can see the correlation between I_{reset} and the on-state resistance. The driving force for filament rupture in URS is usually ascribed to the Joule heating, while, in BRS, it is to the oxidation by ion drift. There exists a threshold energy for RS in current-driven URS and field-induced BRS. For air_760Torr, URS disappears when I_{cc}<3 mA. For O_2_1Torr, a broad dispersion occurs when I_{cc} = 1 mA. This abnormal distribution is attributed to the parasitic capacitance that exists

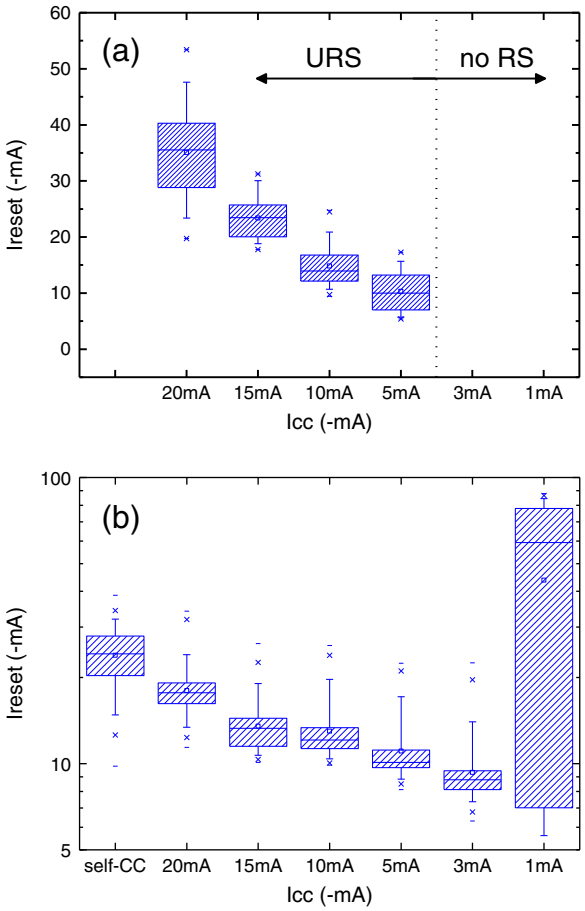

Fig. 3. Effect of compliance current on the reset current. (a) For air_760Torr, (b) for O2_1Torr.

between the device and the external current limiter in 4155A. That would provide a discharge path and result in an overshoot current [16–18].

The XPS spectra of O 1s for all three sets are shown in Fig. 4. The raw data are deconvoluted into two peaks of 530 eV and 531.2 eV, which correspond to the O^{2-} bound to Ti^{4+} and non-lattice oxygen [19]. A number of studies reported that non-lattice oxygen relates to the formation of oxygen vacancy [13], which could modulate the effective Schottky barrier height at the Ag/TiO_2 interface and change the current density [20]. The observation of less non-lattice oxygen in air_760Torr indicates a reduced oxygen vacancy amount, higher interface barrier, and lower current density, and vice versa for O_2_1Torr. The air_760Torr devices thus require the electrical-forming process, and Joule heating could dominate the formation/rupture of the filaments with the diffusion of the oxygen ions. It means the no electroforming process in O_2_1Torr could be attributed to the oxygen vacancy preexisting in films and acting as the conduction path. The non-lattice ion migration to recover the oxygen vacancy during the reset process corresponds to an oxidation reaction. The modulated barrier height near the electrode interface determines the switching mode to be URS or BRS [9,21]. It is inferred that self-compliance in set switching is accompanied by the multiple filaments composed of abundant oxygen vacancies.

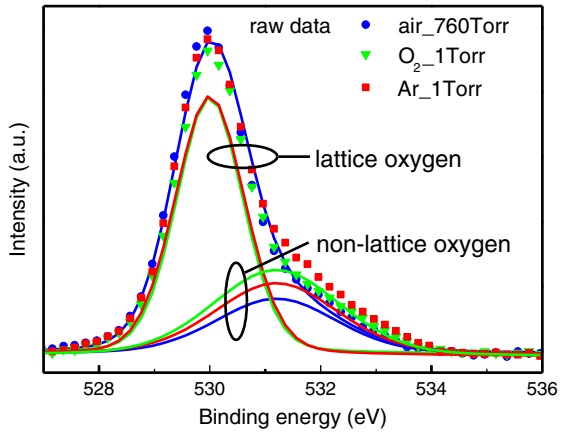

Fig. 4. XPS spectra of O 1s for all the three sets.

Based on XPS analysis, the oxygen vacancy amount seems to be related to the URS/BRS effect, and the change in the switching mode would reflect on the I–V stability and endurance performance. The above statements apply to the comparison between air_760Torr URS and O_2_1Torr BRS, as shown in Fig. 2(a) and (b). For the Ar_1Torr sample, Fig. 5(a) shows its BRS with forming-free and self-compliance in a sequence of 1000 times, and Fig. 5(b) is the endurance test up to 3000 cycles. By examining the higher non-lattice ion content for O_2_1Torr in XPS results, several factors have to be taken into account to explain the endurance improvement for Ar_1Torr. In addition to the oxygen vacancy amount, further research is needed to investigate the effect of metal ion diffusion from top electrode to form multiple filaments, and if the Ar atmosphere is beneficial to the growth of Magneil phase as the conducting nanofilaments [22]. Fig. 6 shows the dispersion comparison of the switching voltage V_{set}/V_{reset} for the three sets. The Ar_1Torr devices demonstrate higher uniformity of operation voltage

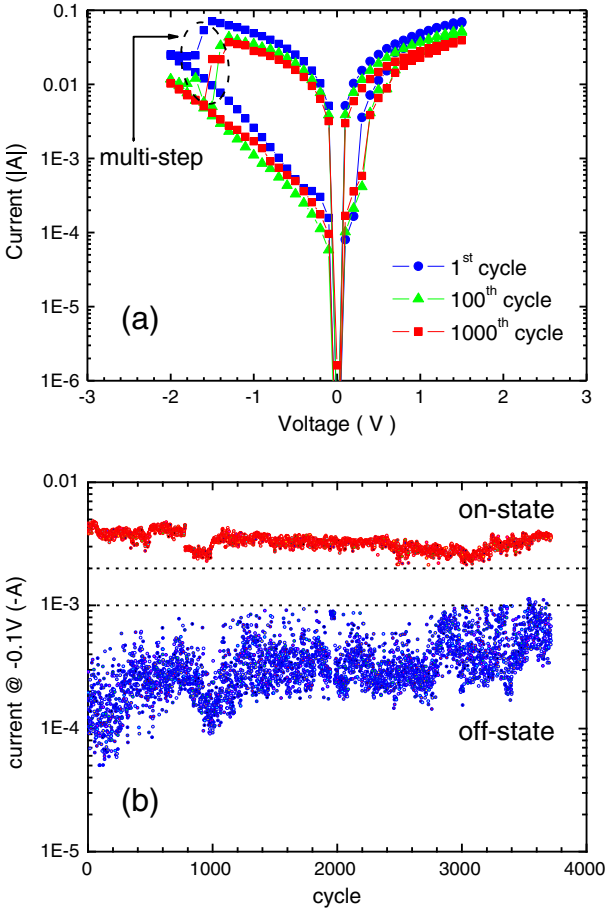

Fig. 5. (a) I–V curves in a continuous switch of 1000 times for Ar_1Torr, (b) the endurance test.

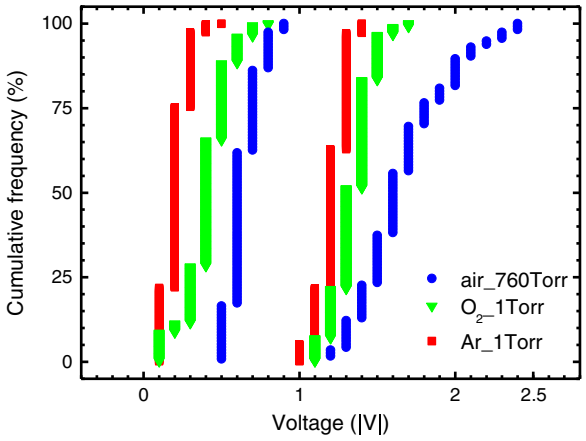

Fig. 6. Comparison of V_{set}/V_{reset} distribution after successive measurements.

and endurance cycles than the other two devices. The dispersion of operation voltage is reduced to be 0.5 V approximately.

The slight difference in the reset transition for Figs. 2(b) and 5(a) is presumed the presence of a multi-step switching behavior. It is indicative of an increasing number of conductive filaments for Ar_1Torr. The filaments are ruptured successively during the turn-off process. The formation of multiple conductive filaments explains why the I–V displays several discrete resistance steps, and could be employed to develop multilevel operation storage [23].

4. Conclusions

Different firing ambience treatment leads to TiO_2 thin films with RS of distinct switching mode and endurance property. The endurance of forming necessary URS by air is near 100 at I_{cc} of 10 mA, and the distribution of the operation voltage is about 1.3 V. While in other two sets by deficient oxygen atmosphere, forming-free and self-compliance BRSs are observed with better stability. XPS analysis reveals the variant non-lattice oxygen peaks, which indicates oxygen vacancy amount present in film interior. The filament formation is facilitated by oxygen vacancy, and the increasing filament number in Ar_1Torr would be helpful in the endurance performance. The endurance is improved to 3000 cycles and dispersion of operation voltage is down to 0.5 V. The TiO_2-based RRAM devices have great potential for multilevel operation storage.

Acknowledgments

The authors thank the National Science Council of the R.O.C. for financial support under project No. NSC-99-2221-E-239-037.

References

[1] S. Seo, M.J. Lee, D.C. Kim, S.E. Ahn, B. Park, Y.S. Kim, I.K. Yoo, I.S. Byun, I.R. Hwang, S.H. Kim, J. Kim, J.S. Choi, J.H. Lee, S.H. Jeon, S.H. Hong, B.H. Park, Appl. Phys. Lett. 87 (2005) 263507.
[2] B.J. Choi, D.S. Jeong, S.K. Kim, C. Rohde, S. Choi, J.H. Oh, H.J. Kim, C.S. Hwang, K. Szot, R. Waser, B. Reichenberg, S. Tiedke, J. Appl. Phys. 98 (2005) 033715.
[3] L. Dongsoo, C. Hyejung, S. Hyunjun, C. Dooho, H. Hyunsang, L. Myoung-Jae, S. Sun-Ae, I.K. Yoo, IEEE Electron Device Lett. 26 (2005) 719.
[4] K.M. Kim, B.J. Choi, Y.C. Shin, S. Choi, C.S. Hwang, Appl. Phys. Lett. 91 (2007) 012907.
[5] U. Russo, D. Ielmini, C. Cagli, A.L. Lacaita, IEEE Trans. Electron Devices 56 (2009) 186.
[6] T. Hou, K. Lin, J. Shieh, J. Lin, C. Chou, Y. Lee, Appl. Phys. Lett. 98 (2011) 103511.
[7] H. Schroeder, D.S. Jeong, Microelectron. Eng. 84 (2007) 1982.
[8] F. Zhang, X.M. Li, X.D. Gao, L. Wu, X. Cao, X.J. Liu, R. Yang, J. Appl. Phys. 109 (2011) 104504.
[9] Y. Shimeng, H.S.P. Wong, IEEE Electron Device Lett. 31 (2010) 1455.
[10] M. Langlet, P. Jenouvrier, A. Kim, M. Manso, M.T. Valdez, J. Sol-Gel Sci. Technol. 26 (2003) 759.
[11] C. Rohde, B.J. Choi, D.S. Jeong, S. Choi, J. Zhao, C.S. Hwang, Appl. Phys. Lett. 86 (2005) 262907.
[12] L.-F. Liu, J.-F. Kang, N. Xu, X. Sun, C. Chen, B. Sun, Y. Wang, X.-Y. Liu, X. Zhang, R.-Q. Han, Jpn. J. Appl. Phys. 47 (2008) 2701.
[13] Q.N. Mao, Z.G. Ji, J.H. Xi, J. Phys. D: Appl. Phys. 43 (2010) 395104.
[14] Z. Fang, H.Y. Yu, X. Li, N. Singh, G.Q. Lo, D.L. Kwong, IEEE Electron Device Lett. 32 (2011) 566.
[15] L. Chang Bum, L. Dong Soo, A. Benayad, L. Seung Ryul, C. Man, L. Myoung-Jae, H. Jihyun, K. Chang Jung, U.I. Chung, IEEE Electron Device Lett. 32 (2011) 399.
[16] S.B. Lee, A. Kim, J.S. Lee, S.H. Chang, H.K. Yoo, T.W. Noh, B. Kahng, M. Lee, C.J. Kim, B.S. Kang, Appl. Phys. Lett. 97 (2010) 093505.
[17] K. Kinoshita, K. Tsunoda, Y. Sato, H. Noshiro, S. Yagaki, M. Aoki, Y. Sugiyama, Appl. Phys. Lett. 93 (2008) 033506.
[18] H.J. Wan, P. Zhou, L. Ye, Y.Y. Lin, T.A. Tang, H.M. Wu, M.H. Chi, IEEE Electron Device Lett. 31 (2010) 246.
[19] K.A. Bogle, M.N. Bachhav, M.S. Deo, N. Valanoor, S.B. Ogale, Appl. Phys. Lett. 95 (2009) 203502.
[20] N. Xu, L. Liu, X. Sun, X. Liu, D. Han, Y. Wang, R. Han, J. Kang, B. Yu, Appl. Phys. Lett. 92 (2008) 232112.
[21] J. Shin, I. Kim, K.P. Biju, M. Jo, J. Park, J. Lee, S. Jung, W. Lee, S. Kim, S. Park, H. Hwang, J. Appl. Phys. 109 (2011) 033712.
[22] D.H. Kwon, K.M. Kim, J.H. Jand, J.M. Jeon, M.H. Lee, G.H. Kim, X.S. Li, G.S. Park, B. Lee, S. Han, M. Kim, C.S. Hwang, Nat. Nanotechnol. 5 (2010) 148.
[23] Q. Liu, C. Dou, Y. Wang, S. Long, W. Wang, M. Liu, M. Zhang, J. Chen, Appl. Phys. Lett. 95 (2009) 023501.